



# Impact of convection on the upper-tropospheric composition (water vapor/ozone) over a subtropical site (Réunion Island, 21.1°S-55.5°E) in the Indian Ocean

5 Damien Héron<sup>1</sup>, Stéphanie Evan<sup>1</sup>, Jérôme Brioude<sup>1</sup>, Karen Rosenlof<sup>2</sup>, Françoise Posny<sup>1</sup>, Jean-Marc Metzger<sup>3</sup> and Jean-Pierre Cammas<sup>1,3</sup>

<sup>1</sup>LACy, Laboratoire de l'Atmosphère et des Cyclones, UMR8105 (CNRS, Université de La Réunion, Météo-France), Saint-Denis de la Réunion, France

<sup>2</sup>Chemical Sciences Division, Earth System Research Laboratory, NOAA, Boulder, CO, USA

10 <sup>3</sup>Observatoire des Sciences de l'Univers de La Réunion, UMS3365 (CNRS, Université de La Réunion, Météo-France), Saint-Denis de la Réunion, France

*Correspondence to:* Damien Héron ([damien.heron@univ-reunion.fr](mailto:damien.heron@univ-reunion.fr))

**Abstract.** Observations of ozonesonde measurements of the NDACC/SHADOZ program and humidity profiles from the daily Météo-France radiosondes at Réunion Island (21.1°S, 55.5°E) from November 2013 to April 2016 are analyzed to identify the origin of wet upper tropospheric air masses with low ozone mixing ratio observed above the island, located in the South West Indian Ocean (SWIO). A seasonal variability in hydration events in the upper troposphere was found and linked to the convective activity within the SWIO basin. In the upper troposphere, ozone mixing ratios were lower (mean of 57 ppbv) in humid air masses (RH>50%) compared to the background mean ozone mixing ratio (73.8 ppbv). A convective signature was identified in the ozone profile dataset by studying the probability of occurrence of different ozone thresholds. It was found that ozone mixing ratios lower than 45 to 50 ppbv had a local maximum of occurrence between 10 and 13km in altitude, indicative of the mean level of convective outflow. Combining FLEXPART Lagrangian backtrajectories with METEOSAT 7 infrared brightness temperature products, we established the origin of convective influence on the upper troposphere above Réunion island. It has been found that the upper troposphere above Réunion island is impacted by convective outflows in austral summer. Most of the time, deep convection is not observed in the direct vicinity of the island, but more than a thousand of kilometers away from the island, in the tropics, either from tropical storms or the Inter Tropical Convection Zone (ITCZ). In November and December, the air masses above Réunion Island originate, on average, from Central Africa and the Mozambique channel. During January, February the source region is the North-east of Mozambique and Madagascar. Those results improve our understanding of the impact of the ITCZ and tropical cyclones on the hydration of the upper troposphere in the subtropics in the SWIO.

## 30 1 Introduction

The variability of ozone in the tropical upper troposphere (10-16 km in altitude) is important for the climate as it influences the radiative budget (Lacis et al. 1990, Thuburn and Craig, 2002), and modifies the oxidizing capacity of the atmosphere and



the lifetime of other chemical species. The tropical ozone budget in the upper troposphere is influenced by stratospheric intrusions, convective transport from the surface, advection from mid-latitudes and chemical reactions.

35 Due to the complex interplay between dynamics and chemistry, tropical ozone concentrations observed by radiosondes at stations within the SHADOZ network show large spatial and temporal variability (Thompson et al., 2003a; Fueglistaler et al., 2009). The average tropical ozone mixing ratio in the upper troposphere has a value of 40 ppbv, varying between 25 to 60 ppbv. Causes for the ozone variability in the tropics are particularly difficult to ascertain without a careful analysis of the processes involved in the observed variability (Fueglistaler et al., 2009). One example is that the S shape found in the mean  
40 ozone profile in the SHADOZ stations over the Pacific, was interpreted by Folkens and Martin (2005) to be a consequence of the vertical profile of the cloud mass flux divergence.

In general, the impact of convection on the ozone budget in the tropical upper troposphere is not well established. Solomon et al. (2005) used a statistical method to characterize the impact of convection on the local ozone minimum in the upper troposphere above the SHADOZ sites within the maritime continent (Fiji, Samoa, Tahiti, and Java). They identified a minimum  
45 of 20 ppbv of ozone in 40% of the ozone profiles. 20 ppbv corresponds also to the ozone mixing ratio in the local oceanic boundary layer. The sites are located in a convectively active region (Hartmann, 1994; Laing & Fritsch, 1997; Solomon et al., 2005; Tissier et al., 2016) and have a higher probability to be influenced by local deep convection than other SHADOZ sites.

Tropical convection can transport air masses from the marine boundary layer to the upper troposphere (Jorgensen and LeMone, 1989; Pfister et al., 2010) in less than a day. Because the ozone chemical lifetime is on the order of 50 days, air masses within  
50 the convective outflow will retain the chemical signature of the boundary layer (Folkens et al., 2002, 2006). Ozone can therefore be used as a convective tracer, and in doing such Solomon et al. (2005) estimated the mean level of convective outflow to be between 300 hPa and 100 hPa, or 8 and 14 km in altitude for SHADOZ stations located in the Western Pacific.

At present, little is known about the impact of convection on SHADOZ sites that are away from active convective regions. In the Southern Hemisphere, the position of Réunion Island (21.1°S-55.5°E) in the South-West Indian Ocean (SWIO, 10°S to  
55 45°S and 40°E to 80°E) is particularly well suited to study the chemical composition of the troposphere over the Indian Ocean. During austral summer (November to April), the Inter Tropical Convergence Zone (ITCZ) moves closer to Réunion Island and convective activity in the SWIO is more pronounced with tropical cyclones forming in the region. Blamey and Reason (2012) estimated that the east of Mozambique Channel is the most convective zone of the region.

In this paper, we analyze ozonesonde measurements of the NDACC/SHADOZ program and humidity profiles from daily  
60 Météo-France radiosondes from Reunion Island between November 2013 and April 2016 to identify the origin of wet upper tropospheric air masses with low ozone mixing ratio observed above the island and understand the role of transport, detrainment, and mixing processes on the composition of the tropical upper-troposphere over Réunion Island. We use infrared brightness temperature data from the METEOSAT 7 geostationary satellite to identify deep convective clouds over the SWIO region. The geographic origin of air masses measured by the radiosondes is estimated using Lagrangian backtrajectories  
65 calculated by the FLEXible PARTicle (FLEXPART) Lagrangian Particle Dispersion Model (Stohl et al., 2005). Section 2 presents the radiosonde measurements, satellite products and FLEXPART model used in this study. Section 3 presents the seasonal variability in ozone/humidity as well as the convective influence on the radiosonde measurements. Results on the mean level of convective outflow and the convective origin of the air masses measured over Réunion Island are also presented in section 3. A summary and conclusions are given in section 4.



## 70 2 Measurements and Model

### 2.1 Ozone and water vapor soundings

The ozonesondes at Réunion Island are launched under the framework of the Network for the Detection of Atmospheric Composition Changes (NDACC) and the Southern Hemisphere ADditional OZonesondes (SHADOZ) programs. The SHADOZ project gathers ozonesonde and radiosonde (pressure, temperature, wind) data from tropical and subtropical stations (Sterling et al., 2018; Witte et al. 2017, 2018; Thompson et al., 2017). Between 2014 and 2016, 158 ozonesondes were launched at Réunion Island (almost 3 per month). The majority of the ozonesonde launches occur around 10 UTC. Balloons carry the ECC ozonesonde (Electrochemical Concentration Cell) in tandem with the Meteomodem M10 meteorological radiosonde. Smit et al. (2007) evaluate ECC-sonde precision to be better than  $\pm (3-5) \%$  and accuracy about  $\pm (5-10) \%$  below 30 km altitude.

80 In addition, we use data from operational daily meteorological Meteomodem M10 radiosondes launches performed by Météo-France (MF) at 12 UTC since 2013. The MF dataset provides RH measurements at a higher frequency than the SHADOZ data and this is important to study the day to day variability of the impact of convection on the upper troposphere. The Meteomodem M10 radiosondes provide measurements of temperature, pressure, relative humidity (RH) and zonal/meridional winds. For both MF and SHADOZ sondes, the average ascent speed of the balloon is 5m/s and measurements are recorded every second  
85 so the mean native vertical resolution is around 5 m for both datasets. Vertical gaps as high as 500 m can occur in the two datasets and the native vertical resolution varies with altitude. Thus NDACC/SHADOZ ozonesonde and MF radiosonde data are interpolated to a regular vertical grid with a 200-m grid spacing.

As noted previously, this study focuses on austral summer conditions (November to April) and in particular the austral summer seasons 2013-2014, 2014-2015, and 2015-2016 (hereafter referred to as summer 2014, 2015 and 2016 respectively). Figure 1  
90 shows the NDACC/SHADOZ 2013-2016 seasonal average ozone mixing ratio profiles as well as the overall mean 4-year average. The 4-year average profile over 2013-2016 increases in the troposphere (from 25 ppbv at the surface to 200 ppbv at 17 km). In austral autumn (March, April and May) and winter (June, July and August) the ozone values are lower than the mean climatology in the troposphere above 3 km. Ozone values increase in the lower troposphere during the dry season (from May to September when biomass burning plumes from southern Africa and Madagascar can be transported eastward and result  
95 in ozone production in the lower troposphere over the Indian Ocean (Sinha et al., 2004). The maximum of tropospheric ozone occurs in austral spring (September, October and November) at the end of the biomass burning season (which extends from July to October, Marengo et al., 1990). Austral summer (DJF) exhibits low ozone values, and in particular, below 3 km and between 9 and 14 km summertime ozone is at an annual low. The source of these low values will be discussed later in this paper.

100

### 2.2 METEOSAT 7 geostationary satellite data

METEOSAT 7 is a geostationary satellite positioned at the longitude 58°E that provides images for the Indian Ocean since December 2005. The Thermal Infrared channel (wavelength 10.5-12.5  $\mu\text{m}$ ) of the Spinning Enhanced Visible and Infrared Imager (SEVIRI) instrument onboard METEOSAT 7, has a temporal resolution of 30 minutes and a horizontal resolution of  
105 5 km at nadir. Here we use METEOSAT 7 hourly infrared brightness temperature product available from the ICARE data archive (<ftp://ftp.icare.univ-lille1.fr>).



We assume black body radiation (Slingo, 2004; Tissier et al., 2016) to estimate the brightness temperature. Young et al. (2013) have classified clouds in the tropics from the CloudSat and MODIS database for one year of observations (2007) over the 30°S-30°N latitude band. They established that cirriform clouds have, on average, higher brightness temperatures than deep convective clouds (respectively 268.5K against 228.5K, Figure 5 of Young et al., 2013). Therefore, we identify deep convective clouds by selecting METEOSAT 7 pixels with brightness temperature lower than 230K.

In order to fold FLEXPART weekly products with METEOSAT 7 infrared brightness temperature data, the latter dataset is interpolated to a regular latitude-longitude grid with a 1° resolution. In addition, for every day between November 2013 and April 2016, we create a map of the deepest convective clouds valid for the previous 7 days by accumulating their positions over the prior week. Thus, for each day we establish maps of Deep Convective Clouds Occurrence (DCCO) valid for the previous week as defined in equation 1.

$$DCCO[d, i, j] = \frac{1}{7 \times 24} \sum_{t=d-6}^d \sum_{h=0}^{23} N_t[h, i, j] \text{ with } N_t[h, i, j] = \begin{cases} 1 & \text{if } T_b < 230 \text{ K} \\ 0 & \text{otherwise} \end{cases} \quad (1)$$

In equation 1, DCCO is a function of the day (d), latitude (i) and longitude (j). The term  $N_t$  is the hourly highest cloud counter and  $T_b$  corresponds to METEOSAT 7 infrared brightness temperature. The weekly product is indicated by the sum between day “d” and day “d-6” (a total of seven days). We normalize DCCO by dividing the two sums in equation 1 by the total number of hourly METEOSAT 7 observations available during a week (i.e. 7x24 images). The mean DCCO map for the period of study (summer seasons between November 2013 and April 2016) is shown on Figure 2.

A weakness of the methodology relates to our treatment convective tower anvils, which may have brightness temperatures colder than 230K. However, we assume that only convective centers correspond to cloud tops with a brightness temperature below 230K. We are using this assumption to identify the deep convective clouds and compare their distribution with the vertical transport from the boundary layer to the upper troposphere calculated by the FLEXPART model.

### 2.3 FLEXPART

To estimate the convective origin of mid to upper tropospheric air masses observed above Réunion Island, we use the FLEXPART Lagrangian particle dispersion model (Stohl et al. 2005). Backtrajectories were calculated every hour at 0.25° resolution between November 2013 and April 2016 using meteorological fields from the ECMWF operational (0.25° x 0.25°) model forecasts, with sub grid motions including convection and turbulence schemes (Stohl et al., 2005 and references therein).

We use FLEXPART to calculate backtrajectories of particles from 3 bins at 1 km interval in the upper troposphere (i.e. 10-11 km, 11-12 km, 12-13 km) above Réunion Island. Vertical bins are defined between 10 and 13 km to trace the lower upper-tropospheric ozone values observed during austral summer on Figure 1. The bins have a horizontal latitude-longitude resolution of 0.1°x0.1°. In every altitude bin, 10 000 trajectories are computed backward in time. Transport and dispersion in the atmosphere are done by the resolved winds and the sub grid turbulent parameterization. Week long backtrajectories are initialized every 3 hours (0000, 0300, 0600, 0900, 1200, 1500, 1800 and 2100 UTC) each day between 1 November 2013 and 31 December 2016. The residence times of particles indicate where and for how long air masses sampled over the observation site have resided in a given atmospheric region (lower troposphere, planetary boundary layer, ...) along the backtrajectories (Stohl et al., 2005). Residence times are computed using the model gridded output domain (1°x1° grid cells) values combining the results of the 8 3-hourly runs to provide a daily estimate of the source regions for air particles. We define the daily fraction



of residence time in the lower troposphere (RTLTL, equation 2), as the residence time of air masses that were in the troposphere below 5 km divided by the total residence time in the troposphere. RTLTL is a function of the day (d), the latitude (i) and longitude (j). The convective origin of an air mass observed in the upper troposphere can be inferred by high values of RTLTL, i.e. the air mass was in the low troposphere below 5 km for a significant amount of time compared to the total residence time spent in the whole troposphere. The threshold at 5 km to define the low troposphere was chosen to take into account the convective transport of air masses from the boundary layer and subsequent in-cloud mixing during the ascent from the lower troposphere to the upper troposphere.

150

$$RTLTL[d, i, j] = \frac{1}{T_{total}} \sum_{z=0}^{5km} \sum_{h=1}^8 T_d[h, i, j, z] \text{ with}$$

$T_d[h, i, j, z]$  = residence time in (i, j, z), for back trajectories initialized the "d" day at "h" hours

$$T_{total}[d] = \sum_{i,j,z} \sum_{h=1}^8 T_d[h, i, j, z] = \text{the total residence time of trajectory initialized the "d" day} \quad (2)$$

### 3 Results

#### 155 3.1 Seasonal variability of relative humidity

Figure 3 shows the time series of vertical profiles of relative humidity (RH) from 2014 to 2016. High RH values (above 80%) observed below 2 km are typical values of the tropical humid marine boundary layer (Folkins and Martins, 2004). The mean value of RH in the upper troposphere (10-13 km) ranges from ~10% during the dry season (austral winter, May to October) to 40% during the wet season (austral summer, November to April) throughout the year. The troposphere between 2 and 10 km shows higher values of RH (mean of 37%) during austral summer than during the austral winter (mean of 15%).

Higher values of RH ~60% from the boundary layer to the upper troposphere can be observed sporadically during austral summer. These higher values of RH are related to convective events (e.g. tropical thunderstorms and/or cyclones) in the vicinity of the island. Other high values of RH (>40%) in the upper troposphere also appear and they do not seem directly connected to local convection over Reunion Island. We define these higher values of RH in the upper troposphere as "upper-tropospheric hydration events". We will later show that these upper-tropospheric hydration events are associated with convective detrainment of air masses in the upper troposphere and their subsequent long-range transport to Réunion Island.

Figure 4 shows the time evolution of RH between 10 and 13 km in altitude. Peak values of RH as high as ~60% are observed. Their occurrence varies from 2014 to 2016. It is known that the El-Niño–Southern Oscillation (ENSO) can affect convective activity over the SWIO (e.g. Ho et al., 2006; Bessafi and Wheeler, 2006). The NOAA Climate Prediction Center Ocean Niño index (ONI, [http://origin.cpc.ncep.noaa.gov/products/analysis\\_monitoring/ensostuff/ONI\\_v5.php](http://origin.cpc.ncep.noaa.gov/products/analysis_monitoring/ensostuff/ONI_v5.php)), which is based on SST anomalies in the Niño 3.4 region, was equal to -0.4 in austral summer 2014 (ENSO neutral conditions), +0.6 in austral summer 2015 (weak El Niño) and +2.2 in austral summer 2016 (strong El Niño). Figure 4 clearly shows that the strong El Niño year (2016) experienced more tropospheric hydration episodes as identified by mean 10-13 km RH greater than 55% than the weak or neutral years did.

170



175 Several studies (e.g. Ho et al., 2006; Bessafi and Wheeler, 2006) have shown that there is a significant effect of ENSO on the  
SWIO convective activity. With an increase in sea surface temperatures (SST) during El Niño events, convective activity over  
the SWIO is enhanced (Klein et al. 1999). At the same time, El Niño events can increase the vertical wind shear over the  
SWIO, which could reduce the intensification of tropical cyclones (Ho et al., 2006) and so increases the number of storms that  
do not reach the tropical cyclone stage (in the SWIO a storm is classified as a tropical cyclone when 10-minute sustained winds  
180 exceed 118 km/h). The differences in humidification in the upper troposphere can also be affected by the Madden Julian  
Oscillation. A clearer explanation on the interplay between MJO and ENSO would require the analysis of additional years,  
and is out of the scope of this study.

Austral summer 2014 (Figs. 3 & 4) is affected by several three tropical cyclone events. Overall, summer 2014 is the driest of  
the three years. Correlated with a higher ONI at +0.6, higher convective activity is observed in austral summer 2015. Two  
185 outflow from tropical cyclones affected Réunion Island: Bansi from January 9 to 19 and Chedza January 13 to 22. Higher  
convective activity was also observed in February and March 2015. In 2016, associated with a strong El Niño event  
(ONI=+2.2), there is an increase in convective activity as compared to austral summers 2014 and 2015. Figure 4 shows that  
austral summer 2016 is associated with higher RH in the upper troposphere. Previous studies have shown a correlation between  
intense El Niño events and an increase in ITCZ precipitation over the SWIO (Yoo et al., 2006, Ho et al. 2006). We will later  
190 show that the majority of the austral summer 2016 upper tropospheric hydration events are associated with the convective  
activity located in the ITCZ.

Figure 5 shows the histogram of RH between 10 and 13 km for the three austral summer periods (2014, 2015 and 2016). We  
choose a RH value of 25% (corresponding to the median of the distribution) to characterize the upper tropospheric background,  
which should be dry without the effect of convective hydration. In the rest of the study, a RH threshold of 50% is used to  
195 isolate upper tropospheric air masses that have likely been affected by deep convection.

### 3.2 Convective influence on the upper troposphere

In this part of the study, we use the NDACC/SHADOZ dataset to analyze the convective influence on air masses observed  
above Réunion Island. The 2013-2016 NDACC/SHADOZ ozone dataset has a mean background value of 81 ppbv in the upper  
troposphere (average ozone mixing ratio between 10 and 13 km). Figure 6 shows the ozone distributions for the lower  
200 troposphere (below 5km, green bars on Figure 6) and the upper troposphere (10-13 km, grey bars on Figure 6). 76.8% of the  
lower tropospheric ozone data have values ranging from 15 to 40 ppbv. These values agree with ozone mixing ratios typically  
observed for air masses in the marine boundary layer (20 ppbv), we note that the values larger than 20 ppbv can be explained  
by mixing with air masses of the tropical troposphere with climatological higher ozone content. In the upper troposphere,  
ozone mixing ratios range from 30 to 110 ppbv (Fig. 6).

205 For the upper troposphere, we further consider the ozone distribution for humid air masses by using a RH threshold of 50%.  
One main mode appears in the ozone distribution for air masses with RH > 50% (blue bars on Figure 6) that is centered around  
45 ppbv (56.4% of data are between 30 and 57.5 ppbv) As explained previously, the mode centered around 45 ppbv in the wet  
distribution may be associated with vertical transport of low-ozone air masses from the marine boundary layer to the upper  
troposphere and subsequent mixing with tropospheric air masses with higher ozone content along their pathway.

210 Ozone mixing ratios higher than 70 ppbv are observed less frequently in the moist upper troposphere (16% of the observations)  
than in the total distribution (43% of the observations). However, the average ozone mixing ratio in the humid upper  
troposphere is on average higher than the ozone mixing ratio observed in the lower troposphere (45 ppbv against 31.7 ppbv



respectively). This again agrees with a convective transport pathway from the marine boundary layer to the upper troposphere and coupled with mixing.

215 As suggested in Figure 2, and later discussed in section 3.5, the deep convection that may commonly influence the upper  
troposphere above Réunion Island is not directly in the vicinity of the island but further north in the ITCZ region. The difference  
in the ozone signature in the low-troposphere (31 ppbv) and directly above Réunion island (45 ppbv) suggests that mixing  
processes occurred during the long-range transport through the upper troposphere enriched in ozone (~81 ppbv) between the  
convective region and Réunion Island. Since the ozone mixing ratio in tropical marine boundary layer is between 15 to 30  
220 ppbv (Folkins et al., 2002), the difference could not be related to enriched low-tropospheric ozone (45ppbv) near the convective  
sources,

### 3.3 Level of convective outflow

Solomon et al. (2005) have studied ozone profiles at several tropical sites in the Southern Hemisphere to characterize the  
impact of deep convection on the ozone distribution in the tropical troposphere. They studied 6 years of measurements (1998  
225 to 2004) from different stations of the SHADOZ network. In Solomon et al. study, 40% of the ozone profiles over the Western  
Tropical Pacific (WTP) stations (Fiji, Samoa, Tahiti, and Java) have ozone mixing ratios lower than 20 ppbv within the upper  
troposphere (10 to 13 km). 20 ppbv of ozone is the average ozone mixing ratio found in the clean marine boundary layer of  
the WTP. The WTP is the most active convective basin of the Southern Hemisphere due to warmer SSTs in this region  
(Hartmann, 1994; Laing & Fritsch, 1997; Solomon et al., 2005; Tissier et al., 2016). Hence, ozone profiles in the WTP have a  
230 higher probability of being influenced by recent and nearby convection than other SHADOZ stations. It explains the weaker  
probability of record ozone mixing ratio below 20 ppbv in the upper troposphere for other stations which are located further  
from the ITCZ region.

Figure 7 shows fractions of the ozone distribution lower than different ozone mixing ratios (25, 40, 45, 50, 55 and 60 ppbv)  
for ozone profiles taken during the summer seasons of 2013 to 2016. A low probability to measure ozone mixing ratios lower  
235 than 25 ppbv is found at the top of the BL. Furthermore, none of the ozone profiles have a mixing ratio lower than 20 ppbv  
between 8 and 13 km, confirming the results of Solomon et al. (2005), and less than 12% have an ozone mixing ratio lower  
than 40 ppbv. However, the fraction of ozone profiles displays a maximum of occurrence for ozone thresholds at 45 (22%),  
50 (27%) and 55 ppbv (35%) between 10 and 13 km, corresponding to the altitude of the mean level of convective outflow  
found in Solomon et al. (2005).

240 We will show in the subsequent sections that the ozone chemical signature of convective outflow diagnosed from Figure 7 is  
mainly associated with air masses detrained from the ITCZ. In comparison to the WTP region, the ITCZ is primarily located  
north of Réunion Island (Schneider 2014), even in austral summer (Fig. 2). Considering that Réunion Island is farther from  
the ITCZ than the stations in the WTP, a longer time for long-range transport to occur is needed from the convective region to  
Réunion island and thus mixing between low-ozone air masses in the boundary layer with higher ozone upper tropospheric air  
245 can explain the values observed in the upper-troposphere over Réunion Island. Moreover, photochemical production of ozone  
during long-range transport after convective entrainment can increase the ozone of an air mass (Wang 1998).



### 3.4 Origin of convective outflow observed above Réunion island

#### 3.4.1 Tropical Cyclone Hellen as a case-study

Hellen was a tropical cyclone that formed in the Mozambique channel and was named on 26 March 2014. It became a category  
250 4 tropical cyclone on the Saffir-Simpson scale on 30 March 2014. Although, tropical cyclone Hellen is not the most influential  
cyclone on the upper troposphere above Réunion island, it is a relevant case-study as it is representative of tropical cyclones  
that form in the Mozambique channel for the SWIO region. In addition, this system had a clear signature in the RH profile in  
the upper troposphere (relative maximum of RH of 60% at 11 km altitude on Figure 8c, red curve).

Patterns of the RTLTL (fraction of residence times in the lower troposphere, see section 2.3 for definition) during the week  
255 before 31 March 2014 for air masses sampled in the upper troposphere above Réunion Island are displayed on Figure 8a.  
RTLTL can be considered as a map of density probability function of origin of the thousands of trajectory particle source  
locations in the lower troposphere. High values of RTLTL (filled contours on Figure 8a) are observed over the Mozambique  
channel and are coincident with the best track of tropical cyclone Hellen (red curve on figures 8a and 8b). Thus, the  
FLEXPART backward trajectories indicate that the air mass sampled on 31 March 2014 above Réunion Island spent a  
260 significant amount of time in the lower troposphere during the previous week while tropical cyclone Hellen was intensifying  
over the Mozambique Channel. Additionally, the high values of RTLTL coincide with a high weekly mean convective cloud  
cover (DCCO see section 2.2 for definition) for the same week (Fig. 8b). The weekly DCCO was higher over the Mozambique  
Channel in agreement with the presence of the tropical cyclone in this region during the week preceding 31 March 2014. The  
two maps of RTLTL and DCCO roughly display the same pattern (maximum above the Mozambique Channel). By combining  
265 the two products of FLEXPART derived RTLTL and METEOSAT 7 DCCO, we can thus infer that the air mass sampled in the  
upper troposphere over Réunion Island on 31 March 2014 was in the lower troposphere over the Mozambique Channel the  
week before. This air mass was located 1500 km away from Réunion Island and was transported from the lower troposphere  
to the upper troposphere by deep convective clouds within tropical cyclone Hellen and was then eastward toward Réunion  
Island. Hence this specific case study illustrates the ability of the FLEXPART model to track the convective origin of air  
270 masses in the upper troposphere above Réunion Island.

#### 3.4.2 Impact of convection on RH variability.

In this section, we will identify which tropical cyclones have influenced the upper troposphere above Réunion Island. We  
display on figure 9 the trajectories of 23 tropical cyclones (8 in 2014, 9 in 2015 and 6 in 2016) that were within a 2100 km  
radius around Reunion Island, representing 74% of tropical cyclones that developed within the SWIO basin between summer  
275 2014 and 2016 (from November 2013 to April 2016). Outside the 2100km radius, the influence of tropical cyclones (TC) on  
Réunion island upper troposphere is found to be limited (not shown).

There is significant variability in the number of SWIO cyclones that traverse (or maybe form in) the Mozambique channel in  
a given year. For 2014 there were 3 (out of 8 for the SWIO), in 2015 2 (out of 9) and for 2016, none (out of 6). Near Réunion  
Island, a similar activity is found during the three summer seasons (about 2 cyclones per year in the direct vicinity of the  
280 island). In 2014, tropical cyclone Bejisa is the only cyclone that directly impacted Réunion Island. During the three austral  
summer seasons of 2014, 2015 & 2016, half of the tropical cyclones formed Northeast of Réunion Island (12 in total).

In order to determine the low tropospheric origin of upper tropospheric air masses observed over Réunion Island during  
summer 2014, 2015 & 2016 (Fig. 3), we integrated the RTLTL gridded over the domain of study ( $1^\circ$  latitude-longitude  
resolution) to define the spatially integrated quantity sRTLTL (Fig. 10). A peak in the time series of sRTLTL in figure 10 means





285 that an event has increased the lower tropospheric origin of air masses measured in the upper troposphere above Réunion  
island. Then, we integrated the values of the RTLTL folded with DCCO (RTLTLxDCCO) to obtain the probability of convective  
origin of each air mass (Fig. 10). When and where this cumulative probability is not null, the product RTLTLxDCCO points at  
the convective events that most likely hydrated the upper troposphere over Réunion Island. If a peak in sRTLTL is correlated  
with a peak in RTLTLxDCCO, it means that the lower-tropospheric origin estimated by correspondes with convective clouds  
290 measured by the METEOSAT 7 satellite. Finally, the cumulative probability is compared to the RH observations over Réunion  
Island (Fig. 10). This comparison identifies the tropical cyclones that have hydrated the upper troposphere over Reunion  
Island, i.e. TCs Bejisa, Colin, Fobane, Hellen and Guito in 2014 (B, C, D, F, H and G: upper panel of Fig. 10); Bansi, Chedza, and  
Haliba in 2015 (B,C and H: middle panel of Figure 10); Corentin and Daya in 2016 (lower panel of Fig. 10). Note the absence  
of soundings between December 26 and 31 prevent diagnosing the influence of A2 in 2015 (0220142015). Among these  
295 cyclones, 5 of them (Bejisa, Fobane in 2014; Bansi, Haliba in 2015; Daya in 2016) had trajectories close to Réunion Island, 5  
of them (Deliwe, Guito, Hellen in 2014; Fundi in 2015 and Chedza in 2016) had trajectories west of Réunion Island, and  
finally only 2 (Colin in 2014 and Corentin in 2016) had a trajectory east of Réunion Island.

For the 3 seasons most of the sRTLTL peaks are consistent with RTLTLxDCCO product, but some convective episodes estimated  
300 by FLEXPART are not consistent with DCCO. As explained in section 3.1, the strong El Niño event in 2016 may have  
influenced the convection over the SWIO. The higher RH variability in 2016 could be associated with isolated smaller  
convective clouds that developed more frequently over the SWIO than the other seasons. The statistical model developed in  
this paper is based on the convective influence integrated over a week, and the resolution of the FLEXPART model  
( $0.25 \times 0.25^\circ$ ) limits the capability of our statistical method to evaluate the influence of isolated convective clouds, which could  
305 contribute to the discrepancies found in 2016.

### 3.4.3 Geographic origin of the convective outflow

Figure 11 shows the monthly averaged maps of the product between DCCO and RTLTL, which represents the probability of  
convective influence from a given region on the upper troposphere above Réunion Island. At the beginning of the austral  
summer seasons (November 2013, 2014 and 2015), the main convective regions that influence the upper troposphere above  
Réunion island are located in central Africa (Congo and Angola). Then from November to January, the influential convective  
310 region moves to the east towards the Mozambique channel. For seasons 2014 and 2015, most of the influential convective  
regions are linked to cyclonic activity. Cyclone Bejisa (B-2014, near Réunion Island) and cyclone Deliwe (D-2014, in the  
Mozambique channel) were the most influential convective events in January 2014. For January 2015, two tropical cyclones  
were active in the SWIO, Bansi (B-2015, near Réunion Island) and Chedza (C-2015, Mozambique channel). In February 2014,  
315 three cyclones formed in the SWIO basin. Despite the short distance from the island, TC Edilson (E-2014) did not have a  
significant influence on the upper troposphere above Réunion Island, while more remote tropical cyclones such as Fobane (F-  
2014, East of the island) and Guito (G-2014, in Mozambique channel) significantly hydrated the upper troposphere above  
Réunion Island. In March 2014, the little patch in the Mozambique channel is directly linked with the TC Hellen (H-2014). In  
February 2015 TC activity decreased and convection over Madagascar hydrated the upper troposphere above Réunion Island.  
320 TC Haliba (H-2015) caused the maximum value of DCCOxRTLTL observed east of Madagascar in March 2015 (red contour  
on Figure 11 for March 2015). There were fewer tropical cyclones (Fig. 10 & 11) that influenced Réunion Island in 2016, but  
there was nonetheless intense convective activity over the SWIO. In austral summer 2016, convective activity was more  
spread across the SWIO and southern Africa.



#### 4 Summary and conclusion

325 We analyzed ozonesonde measurements from the NDACC/SHADOZ program and humidity profiles from the daily Météo-  
France radiosondes at Réunion Island between November 2013 and April 2016 to identify the origin of wet upper tropospheric  
air masses with low ozone mixing ratio observed above the island, located in the subtropics of the SWIO basin.

A seasonal variability in hydration events in the upper troposphere was found. The variability was linked to the seasonal  
variability of convective activity within the SWIO basin. An increase in the convective activity in austral summer 2016 (a  
330 strong El Niño year) compared to austral summers 2014 and 2015 was associated with higher upper tropospheric hydration.  
In the upper troposphere, ozone mixing ratios were lower (mean of 57 ppbv) in humid air masses (RH>50%) compared to the  
background mean ozone mixing ratio (73.8 ppbv).

A convective signature was identified in the ozone profile dataset by studying the probability of occurrence of different ozone  
thresholds. It was found that ozone mixing ratios lower than 45 to 50 ppbv had a local maximum of occurrence near the surface  
335 and between 10 and 13km in altitude, indicative of the mean level of convective outflow, in agreement with Solomon et al.  
(2005) and Avery et al. (2010).

Combining FLEXPART Lagrangian backtrajectories with METEOSAT 7 infrared brightness temperature products, we  
established the origin of convective influence on the upper troposphere above Réunion island. We found that the ozone  
chemical signature of convective outflow above Réunion Island is associated with air masses detrained from the ITCZ located  
340 north of the island and tropical cyclones in the vicinity of the island (2100km around the island). A higher correlation between  
tropical cyclone activity and high upper tropospheric RH values was found in austral summers 2014 and 2015. It was found  
that isolated convection within the ITCZ was more pronounced in 2016 (most likely due to the strong El Niño) and as a result  
the vertical transport associated with these isolated convective clouds were misrepresented in the 0.25x0.25° meteorological  
fields used to drive the FLEXPART model. For austral summers 2014 and 2015, the FLEXPART model is able to trace back  
345 the origin of upper tropospheric air masses with low ozone/high RH signatures to convection over the Mozambique  
Channel/Madagascar and within tropical cyclones.

Hence, it has been found that the upper troposphere above Réunion island is impacted by convective outflows in austral  
summer. Most of the time, deep convection is not observed in the direct vicinity of the island, as opposed to the west Pacific  
sites in Solomon et al. (2005) study, but more than a thousand kilometers away from the island in the tropics either from  
350 tropical storms or the ITCZ. In November and December, the air masses above Réunion Island originate, on average, from  
Central Africa and the Mozambique channel. During January, February the source region is the North-east of Mozambique  
and Madagascar.

The average chemical ozone signature of convective outflow was found to be 45ppbv between 10 and 13km in altitude, which  
differs from the 20 ppbv threshold used in Solomon et al. (2005). The higher threshold can be explained by vertical transport  
355 of low-ozone air masses from the marine boundary layer to the upper troposphere and subsequent mixing with tropospheric  
air masses with higher ozone content along their pathway when advected over more than a thousand kilometers.

#### Data availability



360 METEOSAT 7 data used in this study are available at <http://www.icare.univ-lille1.fr/archive>. The NDACC/SHADOZ ozone measurements for Réunion Island are available at <https://tropo.gsfc.nasa.gov/shadoz/Reunion.html>. The FLEXPART Lagrangian trajectories can be requested from the corresponding author Stephanie Evan ([stephanie.evan@univ-reunion.fr](mailto:stephanie.evan@univ-reunion.fr)).

### Author contributions

365 All authors contributed to the paper. DH wrote the manuscript with contributions from SE, JB, KR, JPC. JMM and FP performed the ozone radiosonde measurements. SE and JB performed the FLEXPART simulations. DE processed the radiosonde and FLEXPART data. All authors revised the manuscript draft.

### Competing interests

The authors declare that they have no conflict of interest.

### Acknowledgments

370 OPAR (Observatoire de Physique de l'Atmosphère à La Réunion, including Maïdo Observatory) is part of OSU-R (Observatoire des Sciences de l'Univers à La Réunion) which is being funded by Université de la Réunion, CNRS-INSU, 720 Météo-France, and the french research infrastructure ACTRIS-France (Aerosols, Clouds and Trace gases Research Infrastructure). This work was supported by the French LEFE CNRS-INSU Program (VAPEURDO).

### References

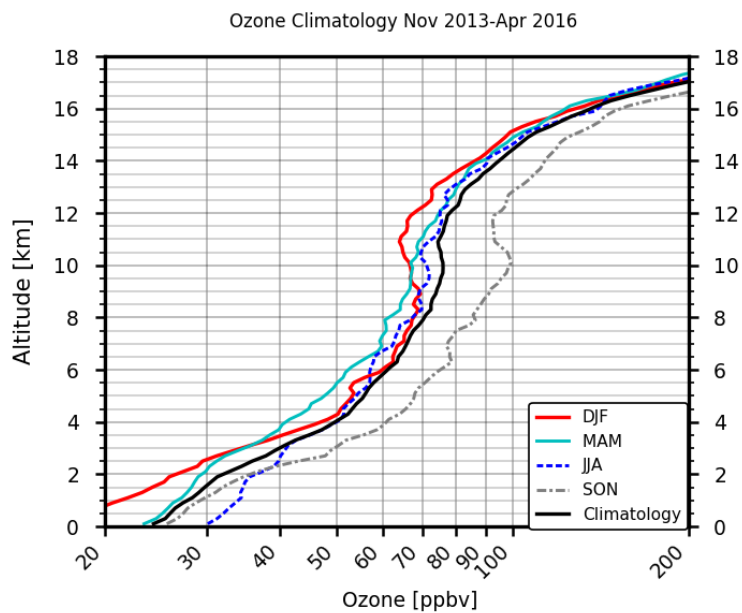
- 375 Avery, M., Twohy, C., McCabe, D., Jioner, J., Severance, K., Atlas, E., Blake, D., Bui, T. P., Crouse, J., Dibb, J., Diskin, G., Lawson, P., McGill, M., Rogers, D., Sashse, G., Scheuer, E., Thompson, A. M., Trepte, C., Wennberg, P., and Ziemke, J.: Convective distribution of tropospheric ozone and tracers in the Central American ITCZ region: Evidence from observations during TC4, *J. Geophys. Res.*, 115, D00J21, doi:10.1029/2009JD013450, 2010.
- Blamey, R. C., and Reason, C. J. C.: Mesoscale Convective Complexes over Southern Africa, *J. Climate*, 25(2), 753-766, doi:10.1175/JCLI-D-10-05013.1, 2012.
- Bessafi, M., and Wheeler, M. C.: Modulation of South Indian Ocean tropical cyclones by the Madden Julian Oscillation and convectively coupled equatorial waves, *Monthly Weather Review*, 134, 638–656, doi:10.1175/MWR3087.1, 2006.
- Folkens, I., Kelly, K. K., and Weinstock, E.M.: A simple explanation for the increase in relative humidity between 11 and 14 km in the tropics., *J. Geophys. Res.*, 4736, doi:10.1029/2002JD002185, 2002.
- 385 Folkens, I., and Martin, R. V.: The vertical structure of tropical convection and its impact on the budgets of water vapor and ozone., *J. Atmos. Sci.*, 62, 1560-1573, <https://doi.org/10.1175/JAS3407.1>, 2005.
- Folkens, I., Bernath, P., Boone, C., Eldering, A., Lesins, G., Martin, R.V., Sinnhuber, B. M., and Walker, K.: Testing convective parameterizations with tropical measurements of HNO<sub>3</sub>, CO, H<sub>2</sub>O, and O<sub>3</sub>: implications for the water vapor budget, *J. Geophys. Res.*, 111, D23304, doi:10.1029/2006JD007325, 2006.
- 390 Fueglistaler, S., Dessler, A., Dunkerton, T., Folkens, I., Fu, Q., and Mote, P.: Tropical tropopause layer, *Rev. Geophys.*, 47, RG1004, doi:10.1029/2008RG000267, 2009.



- Hartmann, D. L., Introduction to Physical Climatology, Academic Press, New York, 411, 1994.
- Ho, C-H, Kim, J-H, Jeong, J-H, Kim, H-S, Chen, D-Y: Variation of tropical cyclone activity in the South Indian Ocean: El Niño-Southern Oscillation and Madden-Julian Oscillation effects, *J. Geophys. Res.*, 111, D22101, doi:10.1029/2006JD007289, 2006.
- Jorgensen, D. P., and Lemone, M. A.: Vertical velocity characteristics of oceanic convection, *J. Atmos. Sci.*, 46, 621-640, [https://doi.org/10.1175/1520-0469\(1989\)046<0621:VVCOOC>2.0.CO;2](https://doi.org/10.1175/1520-0469(1989)046<0621:VVCOOC>2.0.CO;2), 1989.
- Klein, S. A., B. J. Soden, and N.-C. Lau: Remote sea surface temperature variations during ENSO: Evidence for a tropical atmospheric bridge, *J. Climate*, 12, 917-932, [https://doi.org/10.1175/1520-0442\(1999\)012,0917:RSSTVD.2.0.CO;2](https://doi.org/10.1175/1520-0442(1999)012,0917:RSSTVD.2.0.CO;2), 1999.
- 400 Lacis, A. A., Wuebbles, D. J., and Logan, J. A.: Radiative forcing of climate by changes in the vertical distribution of ozone, *J. Geo-phys. Res.*, 95, 9971-9981, 1990.
- Laing, A.G. and Fritsch, J.M.: The global population of mesoscale convective complexes, *Q. J. R. Meteorol. Sue.*, 123, 389-405, 1997.
- Marenco, A., Medale, J. C., and Prieur, S.: Study of tropospheric ozone in the tropical belt (Africa, America) from STRATOZ and TROPOZ campaigns, *Atmos. Environ.*, 24, 2823-2834, 1990.
- 405 Pfister, L., Selkirk, H. B., Starr, D. O., Rosenlof, K., and Newman, P. A.: A meteorological overview of the TC4 mission, *J. Geophys. Res.*, 115, D00J12, doi:10.1029/2009JD013316, 2010.
- Schneider, T., Bischoff, T., and Haug, G. H.: Migrations and dynamics of the intertropical convergence zone, *Nature*, 513, 45-53, doi:10.1038/nature13636, 2014.
- 410 Sinha, P., Jaeglé, L., Hobbs, P. V., and Liang, Q.: Transport of biomass burning emissions from southern Africa, *J. Geophys. Res.*, 109, D20204, doi:10.1029/2004JD005044, 2004.
- Slingo, A., Hodges, K. I., and Robinson, G. J.: Simulation of the diurnal cycle in a climate model and its evaluation using data from Meteosat 7, *Quart. J. Roy. Met. Soc.*, 130, 1449-1467, doi:10.1256/qj.03.165, 2004.
- 415 Solomon, S., Thompson, D. W. J., Portmann, R. W., Oltmans, S. J., and Thompson, A. M.: On the distribution and variability of ozone in the tropical upper troposphere: Implications for tropical deep convection and chemical-dynamical coupling, *Geophys. Res. Lett.*, 32, L23813, doi:10.1029/2005GL024323, 2005.
- Sterling, C. W., Johnson, B. J., Oltmans, S. J., Smit, H. G. J., Jordan, A. F., Cullis, P. D., Hall, E. G., Thompson, A. M., and Witte, J. C.: Homogenizing and estimating the uncertainty in NOAA's long-term vertical ozone profile records measured with the electrochemical concentration cell ozonesonde, *Atmos. Meas. Tech.*, 11, 3661-3687, [https://doi.org/10.5194/amt-11-3661-](https://doi.org/10.5194/amt-11-3661-2018)  
420 2018, 2018.
- Stohl, A., Forster, C., Frank, A., Seibert, P., and Wotawa, G.: Technical note: The Lagrangian particle dispersion model FLEXPART version 6.2., *Atmos. Chem. Phys.*, 5, 2461-2474, doi:10.5194/acp-5-2461-2005, 2005.
- Thuburn, J. and Craig, G. C.: On the temperature structure of the tropical stratosphere, *J. Geophys. Res.*, 107, 4017, doi:10.1029/2001JD000448, 2002.
- 425

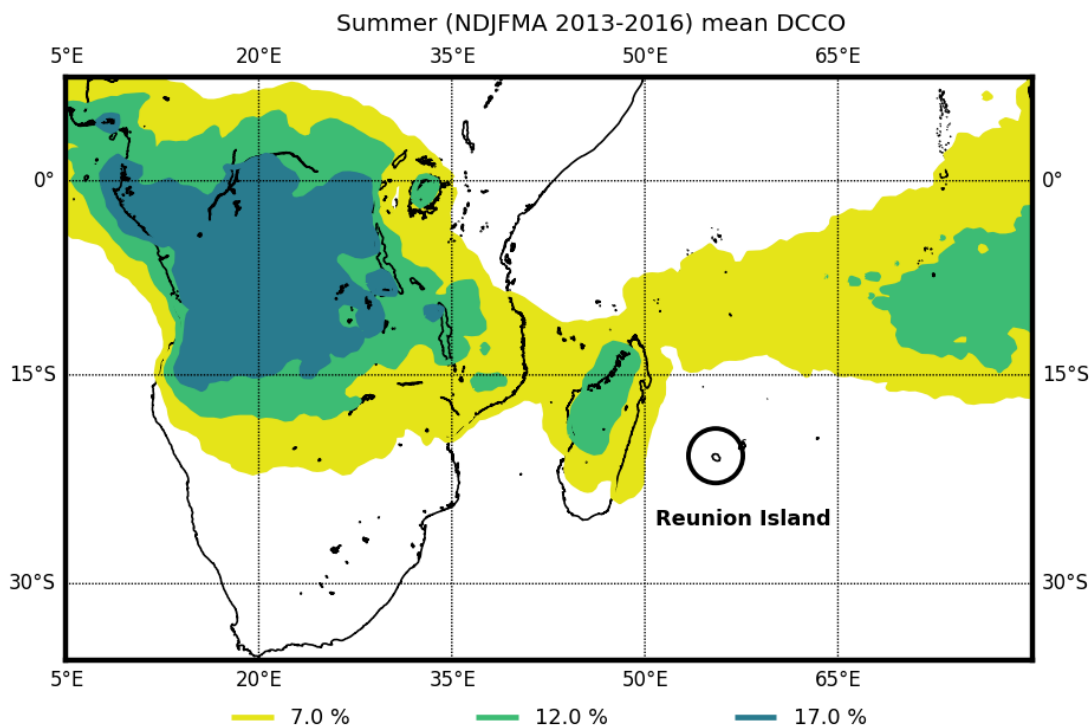


- Tissier, A. S.: Transport au niveau de la tropopause tropicale et convection, Ph.D. thesis, Laboratoire de météorologie dynamique, Université Pierre et Marie Curie - Paris VI, France, 2016.
- Thompson, A. M., Witte, J. C., McPeters, R. D., Oltmans, S. J., Schmidlin, F. J., Logan, J. A., Fujiwara, M., Kirchhoff, V. W. J. H., Posny, F., Coetzee, G. J. R., Hoegger, B., Kawakami, S., Ogawa, T., Johnson, B. J., Vömel, H., and Labow, G.: Southern Hemisphere Additional Ozonesondes (SHADOZ) 1998–2000 tropical ozone climatology 1. Comparison with Total Ozone Mapping Spectrometer (TOMS) and ground-based measurements, *J. Geophys. Res.*, 108(D2), 8238, doi:10.1029/2001JD000967, 2003a.
- Thompson, A., Witte, J., Sterling, C., Jordan, A., Johnson, B., Oltmans, S., Fujiwara, M., Vömel, H., Allaart, M., Piders, A., Coetzee, G. J. R., Posny, F., Corrales, E., Diaz, J., Félix, C., Komala, N., Lai, N., Maata, M., Mani, F., Thiongo, K.: First Reprocessing of Southern Hemisphere Additional Ozonesondes (SHADOZ) Ozone Profiles (1998–2016). 2. Comparisons with Satellites and Ground-based Instruments: SHADOZ Data Evaluation, *J. Geophys. Res.*, 122, 13,000–13,025, doi:10.1002/2017JD027406, 2017.
- University Lille, CNES, CNRS, EU, NASA, INSU, USTL, ICARE Cloud-Aerosol-Water-Radiation Interactions Data Products, ICARE, <ftp://ftp.icare.univ-lille1.fr>, 2014.
- Wang, Y., Jacob, D. J., Logan, J. A.: Global simulation of tropospheric O<sub>3</sub>-NO<sub>x</sub>-hydrocarbon chemistry. 3. Origin of tropospheric ozone and effects of nonmethane hydrocarbons, *J. Geophys. Res.*, 103, 10 757–10 767, 1998.
- Witte J. C., Thompson, A. M., Smit, H. G. J., Fujiwara, M., Posny, F., Coetzee, G. J. R., Northam, E. T., Johnson, B. J., Sterling, C. W., Mohammed, M., Ogino, S.-Y., Jordan, A., daSilva, F. R., and Zainal, Z.: First reprocessing of Southern Hemisphere Additional Ozonesondes (SHADOZ) profile records (1998–2015) 1: Methodology and evaluation, *J. Geophys. Res.*, 122, 6611–6636, <https://doi.org/10.1002/2016JD026403>, 2017.
- Witte, J. C., Thompson, A. M., Smit, H. G. J., Vömel, H., Posny, F., and Stuebi, R.: First reprocessing of Southern Hemisphere Additional Ozonesondes (SHADOZ) Profile Records. 3. Uncertainty in ozone profile and total column, *J. Geophys. Res.*, 123, 3243–3268, <https://doi.org/10.1002/2017JD027791>, 2018.
- Yoo, S. H., Yang, S., and Ho, C. H.: Variability of the Indian Ocean sea surface temperature and its impacts on Asian-Australian monsoon climate, *J. Geophys. Res.*, 111, D03108, doi:10.1029/2005JD006001, 2006.
- Young, A. H., Bates, J. J., and Curry, J. A.: Application of cloud vertical structure from CloudSat to investigate MODIS-derived cloud properties of cirriform, anvil, and deep convective clouds, *J. Geophys. Res. Atmos.*, 118, 4689–4699, doi:10.1002/jgrd.50306, 2013.



455

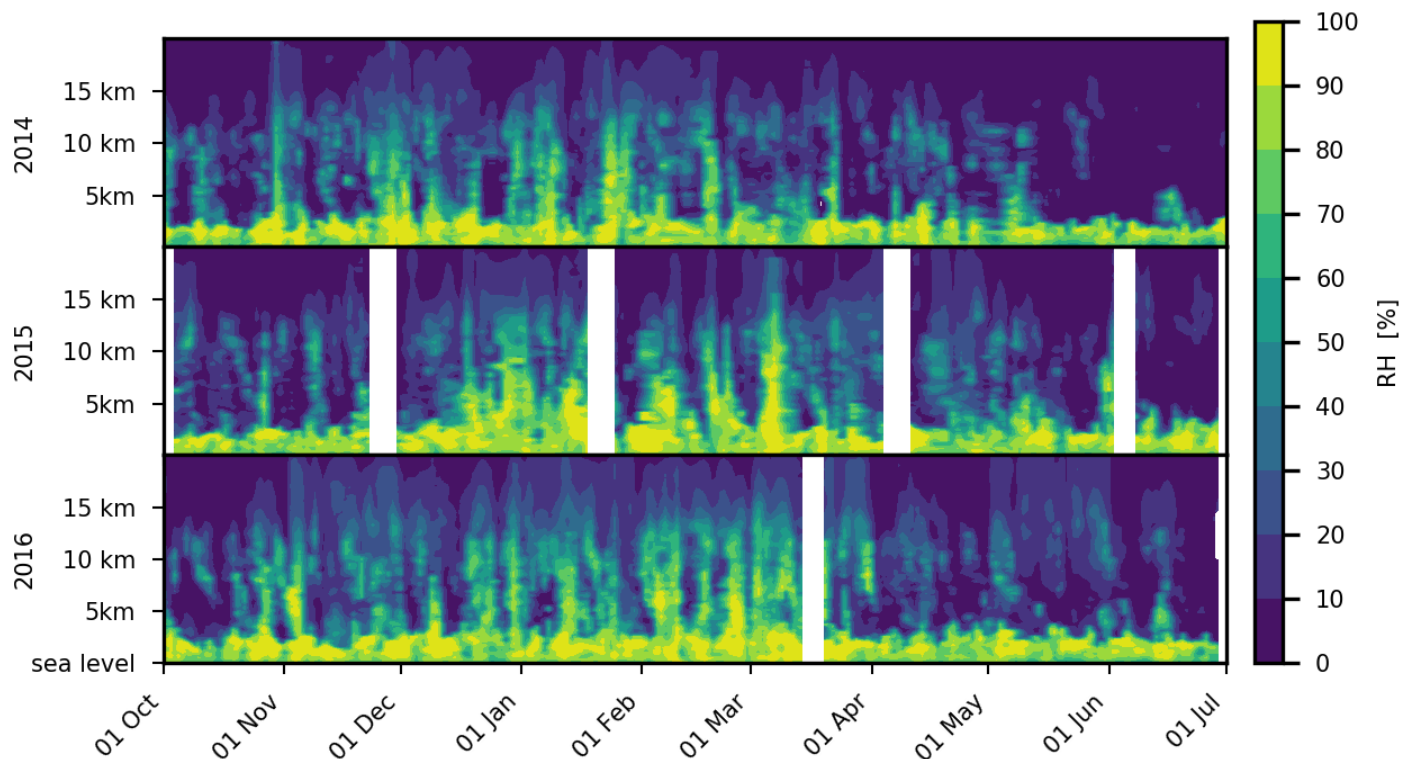
**Figure 1: Climatological mean ozone profile (from November 2013 to April 2016) in black. 2013-2016 seasonal mean ozone profile for summer (December, January, February) in red, spring (March, April, May) in cyan, winter (June, July, and August) in blue and autumn (September, October, November) in grey.**



460 **Figure 2:** Average map of the deepest convective cloud occurrence (DCCO) for austral summer conditions (NDJFMA from November 2013 to April 2016). The yellow contours is for DCCO > 7%, the green contour for DCCO > 12% and the dark green contour is for DCCO > 17%.



### RH evolution



465 **Figure 3: Time height cross-sections of day-to-day variations of Relative Humidity (RH) for Oct 2013-July 2014 (upper panel), Oct 2014-July 2015 (middle panel) and Oct 2015-July 2016 (bottom panel). The RH field is interpolated in time except when 5 days of data are missing.**



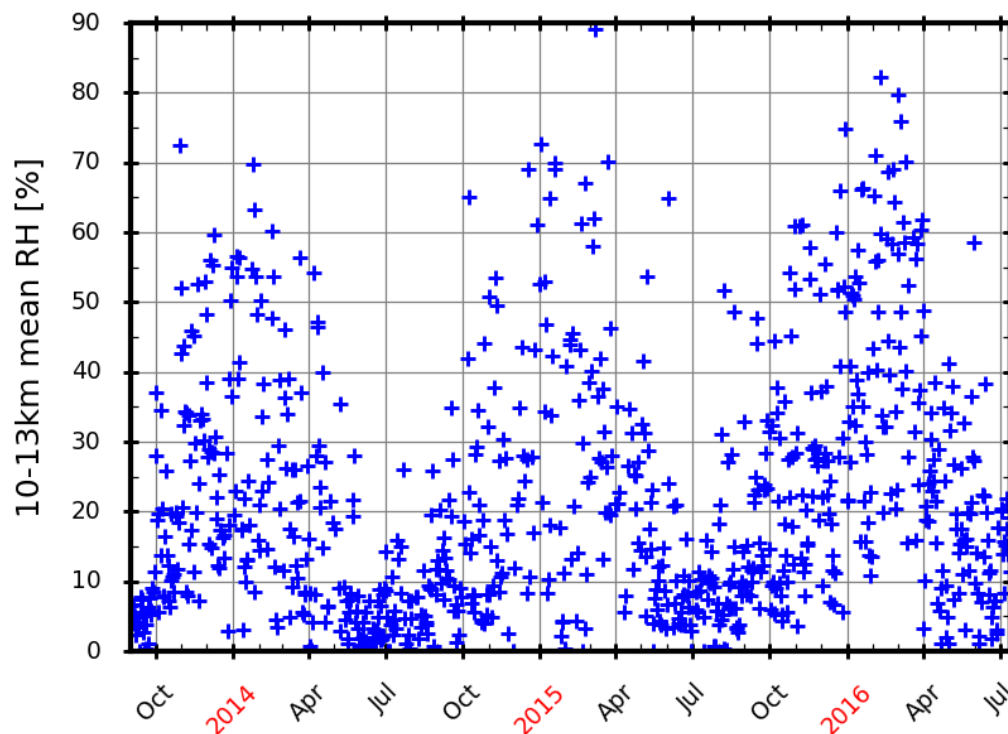
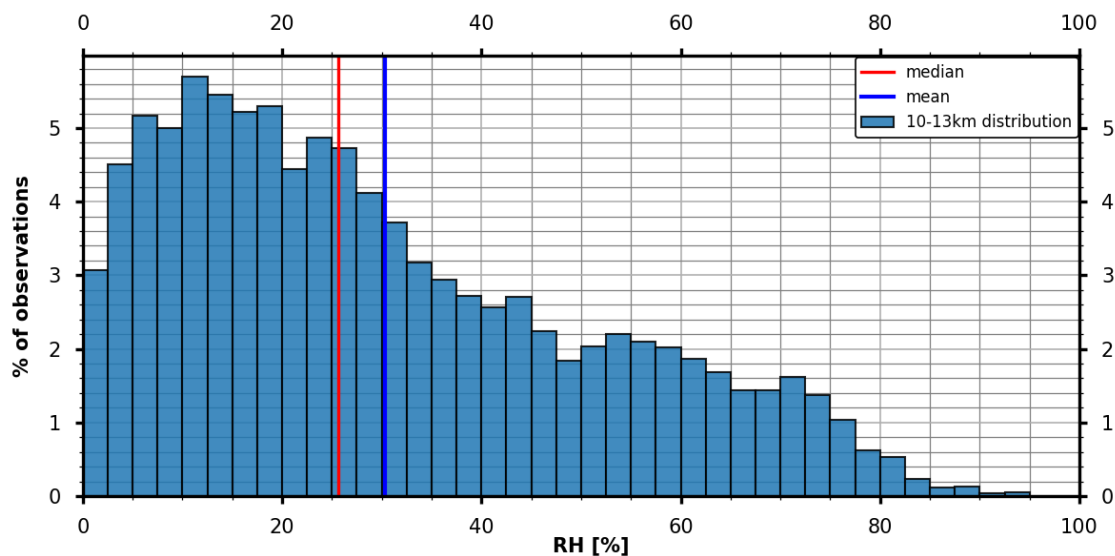


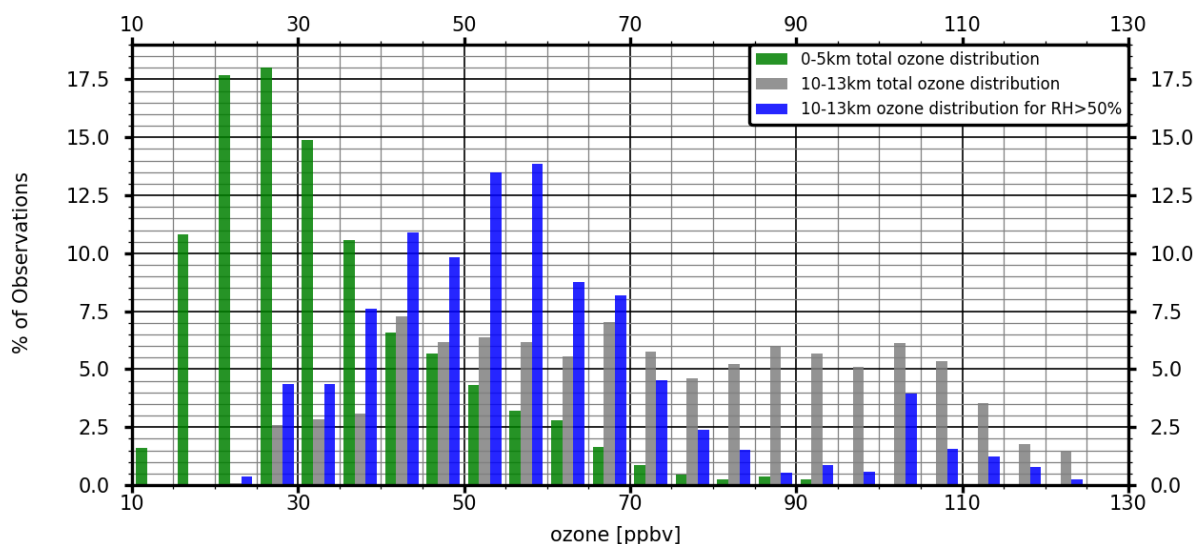
Figure 4: Daily evolution of mean upper tropospheric (10 to 13 km) RH for the period September 2013 to July 2016.



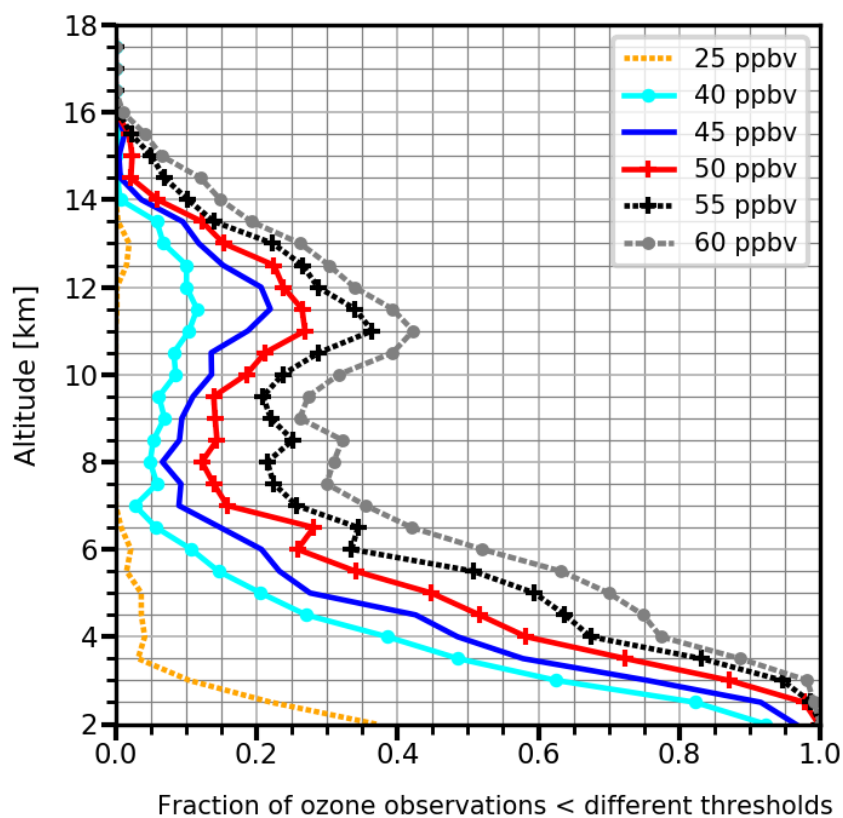
470



**Figure 5:** RH distribution in the upper troposphere (10-13km) above Réunion Island. 904 profiles for the period Nov 2013-Apr 2016 have been used to compute the distribution. Bins are every 5%. The red line shows the median of the distribution ~25%, and the mean RH (in blue) is equal to 30.4%.



475 **Figure 6:** NDACC/SHADOZ ozone distribution in the low troposphere (0-5 km, in green). The total distribution in the upper troposphere (10-13km, in grey) and for moist data (10-13km and RH>50%, in blue). The distributions are based on 55 ozone profiles for austral summers 2014, 2015 and 2016. The mean for each distribution is 73.8 ppbv, 57 ppbv, 33.5 ppbv for the 10-13 total ozone distribution, 10-13 km ozone distribution with RH>50% and 0-5km total ozone distribution respectively.



480 **Figure 7: Vertical profiles of frequency of occurrence of ozone mixing ratios below 25, 40, 45, 50, 55 and 60 ppbv at Réunion Island for austral summers (NDJFMA) 2014, 2015 and 2016**

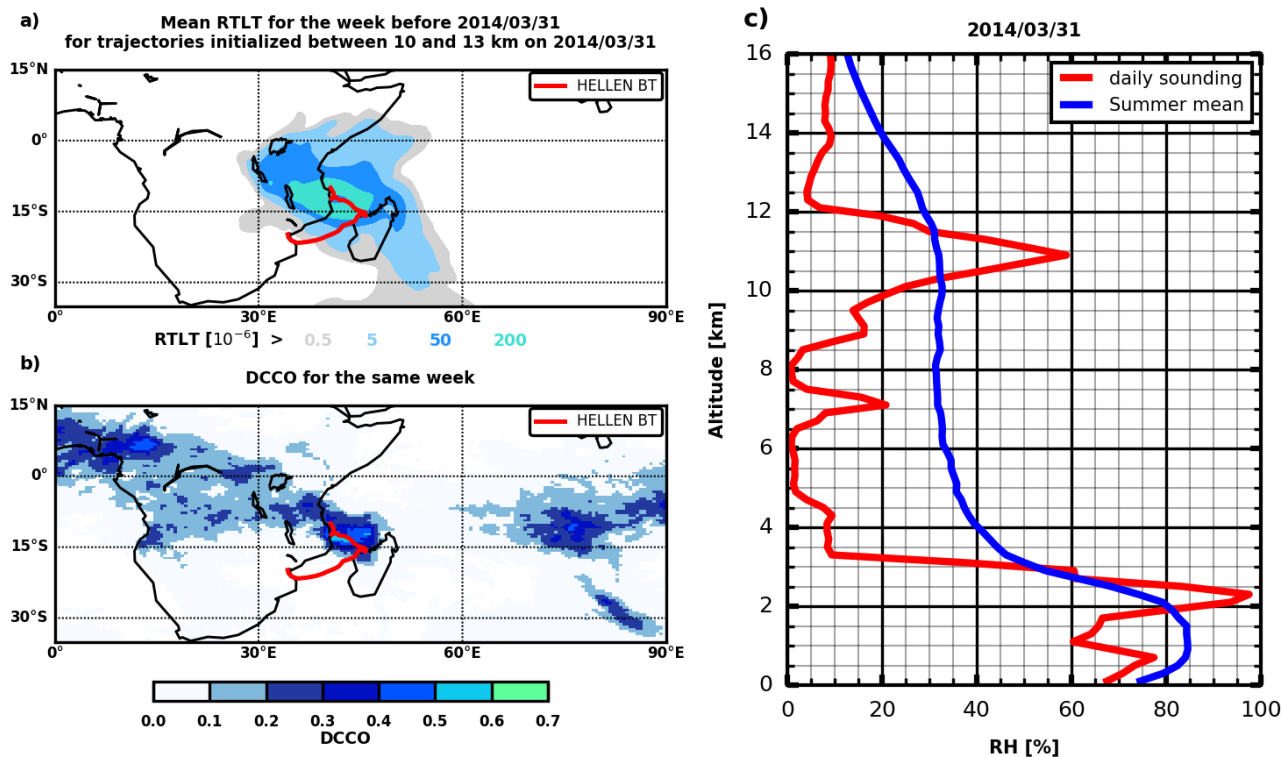
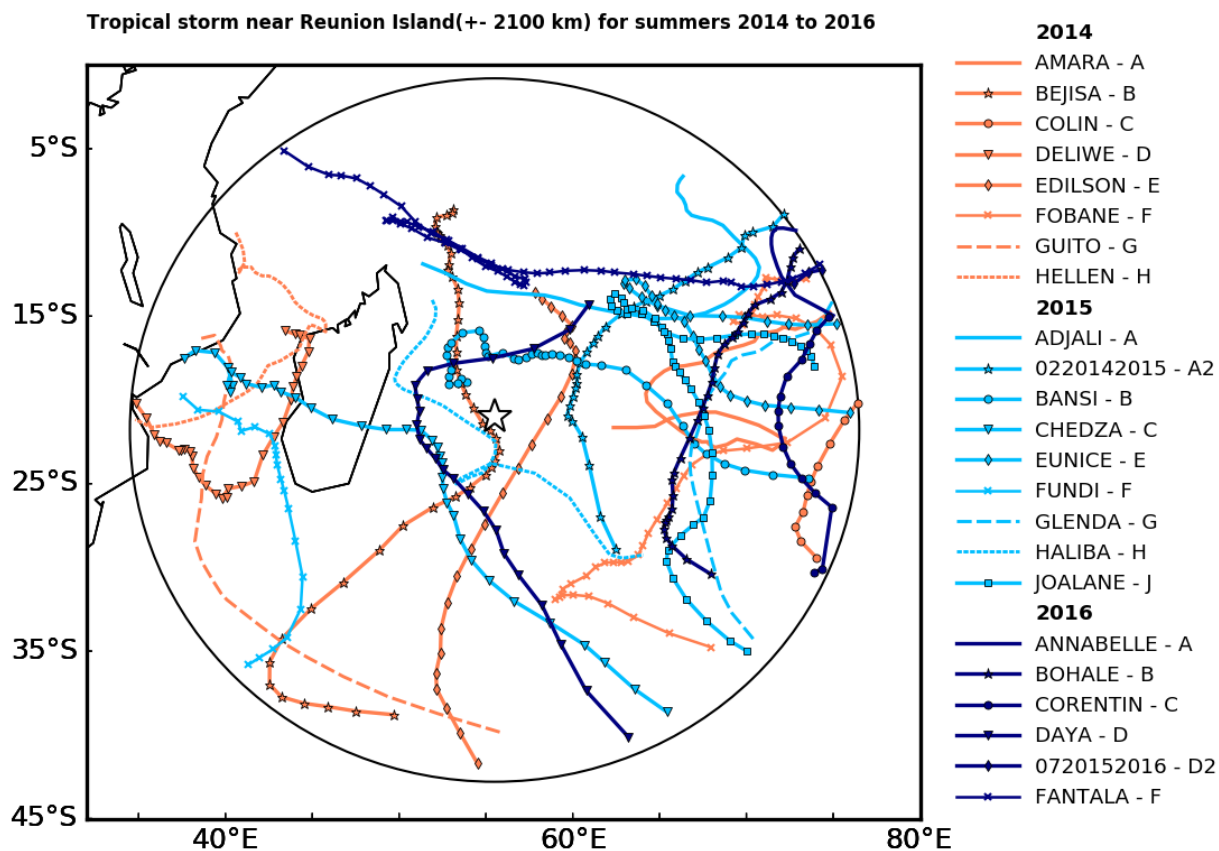
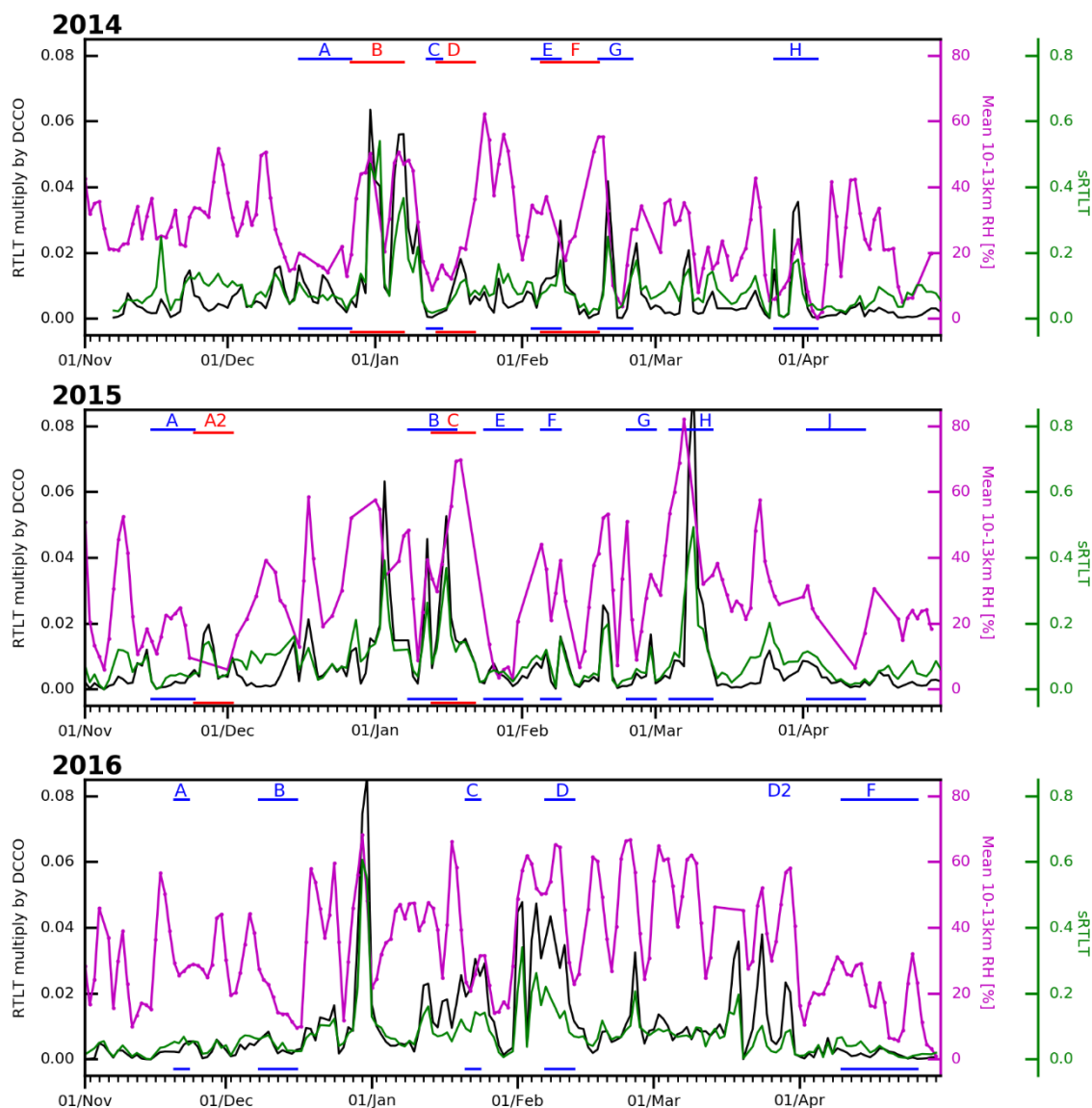


Figure 8:

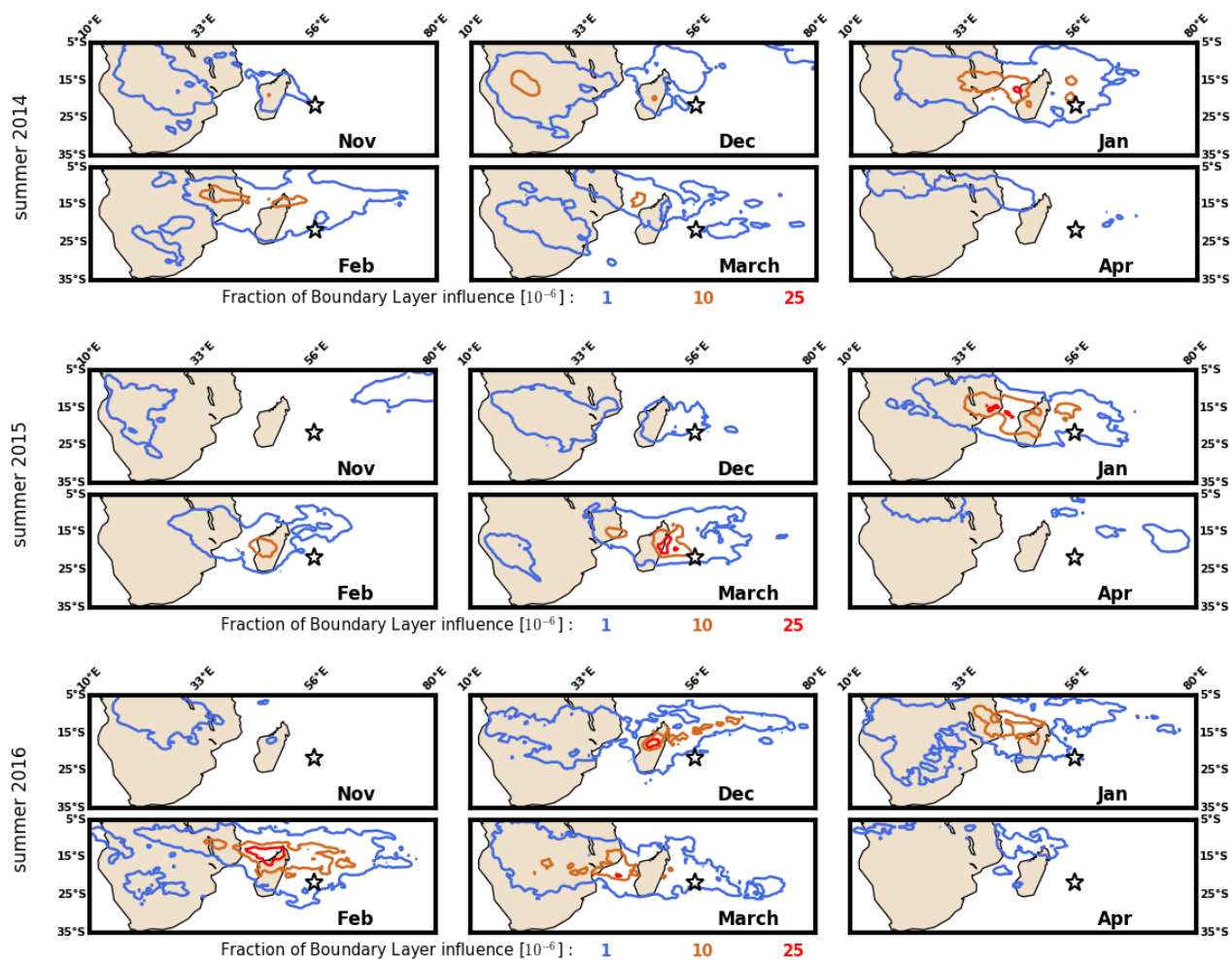
- 485 a) (top-left) fraction of residence time below 5km (RTLTL) for air masses initialized in the upper troposphere (10-13km) over Réunion Island on 31 March 2014
- b) (bottom left) Map of DCCO for the week before 31 March 2014. On (a) and (b) the best-track data are provided by Météo-France.
- c) (right) RH profile on 31 March 2014 in red and seasonal mean RH profile (in blue) for austral summers 2014, 2015 and 2016.



490 **Figure 9:** Map of Tropical Cyclone's best-tracks for a range ring of 2100 km around Réunion Island. The best-tracks of tropical Cyclones during austral summer 2014 (November 2013 to April 2014) are shown in orange with different symbols for each TC, best-tracks for austral summer 2015 (November 2014-April 2015) are in cyan and in blue for austral summer 2016 (November 2015-April 2016, in green). The yellow star indicates the location of Réunion Island.



495 **Figure 10:** Top panel: Time-evolution of sRTLTL (RTLTL spatially summed) in green, product of DCCO by RTLTL in black and mean upper-tropospheric (10-13km) RH in purple for austral summer 2014. Middle and bottom panels: Same as top panel for austral summers 2015 and 2016 respectively. The letters in red and blue indicate periods with different tropical cyclones for each austral summer as shown on Figure 9.



500 **Figure 11: Monthly average product of DCCO by RTL normalized by the total residence time in the whole atmospheric column. From top right to bottom left: November 2013, December 2013, January 2014, February 2014, March 2014, April 2014, November 2014, December 2014, January 2015, February 2015, March 2015 and April 2015. The values for each contour are indicated by the numbers in green, cyan, pink and red at the bottom of the figure. The location of Réunion Island is indicated by a white star on each plot.**